

Dynamical Downscaling over the Great Lakes Basin of North America Using the WRF Regional Climate Model: The Impact of the Great Lakes System on Regional Greenhouse Warming

JONATHAN GULA AND W. RICHARD PELTIER

Department of Physics, University of Toronto, Toronto, Ontario, Canada

(Manuscript received 12 July 2011, in final form 13 May 2012)

ABSTRACT

The Weather Research and Forecasting model (WRF) is employed to dynamically downscale global warming projections produced using the Community Climate System Model (CCSM). The analyses are focused on the Great Lakes Basin of North America and the climate change projections extend from the instrumental period (1979–2001) to midcentury (2050–60) at a spatial resolution of 10 km. Because WRF does not currently include a sufficiently realistic lake component, simulations are performed using lake water temperature provided by D.V. Mironov's freshwater lake model "FLake" forced by atmospheric fields from the global simulations. Results for the instrumental era are first compared with observations to evaluate the ability of the lake model to provide accurate lake water temperature and ice cover and to analyze the skill of the regional model. It is demonstrated that the regional model, with its finer resolution and more comprehensive physics, provides significantly improved results compared to those obtained from the global model. It much more accurately captures the details of the annual cycle and spatial pattern of precipitation. In particular, much more realistic lake-induced precipitation and snowfall patterns downwind of the lakes are predicted. The midcentury projection is analyzed to determine the impact of downscaling on regional climate changes. The emphasis in this final phase of the analysis is on the impact of climate change on winter snowfall in the lee of the lakes. It is found that future changes in lake surface temperature and ice cover under warmer conditions may locally increase snowfall as a result of increased evaporation and the enhanced lake effect.

1. Introduction

Recent studies of the Great Lakes region and surrounding areas have demonstrated that significant changes in temperature and precipitation have occurred during the twentieth century (Vincent and Mekis 2006). Further changes are likely expected to occur in response to continuing increases in CO₂ and other greenhouse gas emissions during the current century. The Great Lakes, as the largest single accumulation of freshwater in the world in a region with over 35 million inhabitants living within their watershed, are vital to the economies of both the United States and Canada. How this region will be impacted by the ongoing process of global warming is clearly of significant interest.

Large freshwater systems such as the Great Lakes play a key role in determining the climate of their basins and adjacent regions by airmass modification through the exchange of heat and moisture with the atmosphere. They significantly affect the structure of the atmospheric boundary layer and therefore the surface fluxes of heat, water vapor, and momentum, which may influence the regional climate in many ways. A major effect of the lakes is to moderate maximum and minimum temperatures of the region in all seasons. They provide a significant source of warmth to the atmosphere during colder seasons and conversely cool the region in summer because of the lag in the cooling of lake waters compared to land surfaces. The seasonal cycle of precipitation is also greatly modified by the presence of the Great Lakes. Precipitation and snowfall are enhanced over and downwind of the lakes during winter by the rapid modification of cold air masses passing over the warm waters of the lakes. The transfer of heat and moisture to cold and dry polar air flowing over the lakes results in heavy snowfall

Corresponding author address: Jonathan Gula, Department of Physics, University of Toronto, 60 St George St., Toronto ON M5S 1A7, Canada.
E-mail: gula@atmosphysics.utoronto.ca

on the lee side of the lakes in areas referred to as snowbelts. On the other hand, convective clouds and rainfall may decrease over the lakes in summer because of the greater atmospheric stability imparted by the relatively cooler water (Scott and Huff 1996).

The role of ice cover is of particular importance as it is known to have a significant effect on both regional climate and weather events [see Brown and Duguay (2010) and references therein]. The presence of ice cover on lakes strongly modifies their interaction with the atmosphere, which makes the timing of lake freeze-up and ice break-up crucial for the simulation of local climate variability and change. Mishra et al. (2011), who studied small inland lakes in the Great Lakes region during the past century, concluded that a significant increase ($0.08\text{--}0.21^{\circ}\text{C decade}^{-1}$) in air temperature resulted in a significant change ($0.2\text{--}2.0$ days decade^{-1}) in lake ice freeze-up and break-up dates. Projected climate warming will likely exert severe impacts on lake ice phenology, with the potential of further increasing the role of lakes (Brown and Duguay 2010). Recent studies of snowfall records in and outside of the Great Lakes region have indicated a significant increase in snowfall in the Great Lakes region during the twentieth century, but no such increase in non-Great Lakes areas (Burnett et al. 2003). Later results could not identify a clear trend for Lakes Erie and Ontario, but confirmed an upward trend in snowfall and liquid precipitation in the Lake Superior and Lake Michigan snowbelts (Kunkel et al. 2009). They suggested that following an upward trend in temperature, the warmer surface water and the decline in ice cover might result in enhanced fluxes of heat and moisture and contribute to the observed upward snowfall trends.

The most recent generation of general circulation models (GCMs) has proven capable of simulating many aspects of large-scale global climate change and variability (Solomon et al. 2007). The applicability of GCM data to climate impact studies, however, is limited by the fact that regional scales are still not well resolved by such global models. Because of limitations in computational resources, existing GCMs typically run at horizontal grid intervals on the order of 200 km, which is far too coarse for applications at regional or local scales of 10–30 km (Leung et al. 2003; Wang et al. 2004; Giorgi 2006) as they cannot capture the effects of geographically localized features such as mountain ranges, complex land–water distributions, or regional variations in land use. A major question is whether such mesoscale heterogeneity at the earth's surface will significantly alter the local temperature and precipitation trends under climate change from those predicted by a model that does not specifically resolve these features.

The nested regional climate modeling (RCM) technique, also referred to as dynamical downscaling, has been developed in an attempt to mitigate this problem. It has become a useful approach for obtaining high-resolution regional climate information from global GCM output (Fowler et al. 2007; Solomon et al. 2007) and improving the credibility of downscaled future climate projections (Liang et al. 2008). The RCM is not intended to modify the large-scale circulation of the GCM but is intended rather to add regional detail in response to regional-scale forcing as it interacts with the larger-scale atmospheric circulation and to reduce biases through a more realistic physics representation (Liang et al. 2006).

To investigate the regional climate changes to be expected over the Great Lakes Basin of North America during the next century, we have performed new century-scale climate simulations at a high resolution of 10 km using the Weather Research and Forecasting (WRF) model as an RCM and the National Center for Atmospheric Research (NCAR) Community Climate System Model 3.0 (CCSM3) as a GCM. As WRF does not currently include a sufficiently realistic lake component, simulations are performed using lake water temperature provided by the freshwater lake model “FLake” (Mironov 2008) forced by atmospheric fields from the global simulations.

The paper is organized as follows. The regional climate model and the experimental configuration are described in section 2. The ability of the model to realistically simulate atmospheric surface fields for the modern instrumental era is presented in section 3. Projections for a mid-twenty-first-century future scenario are given in section 4. Changes in surface temperatures and ice cover for the Great Lakes under future atmospheric conditions are described, and the trends in temperature and precipitation for the future regional climate are discussed in view of these effects. Conclusions of the study are offered and discussed in section 5.

2. Model description and experimental design

a. The global model of climate system evolution: CCSM3

The global GCM to be employed for the purpose of the analyses to follow is the NCAR Community Climate System Model version 3.0. This model is a fully coupled, global climate model that provides simulations of the earth's climate system and that was featured prominently in the Intergovernmental Panel on Climate Change Fourth Assessment Report (IPCC AR4; Solomon et al. 2007). It is composed of four separate models describing

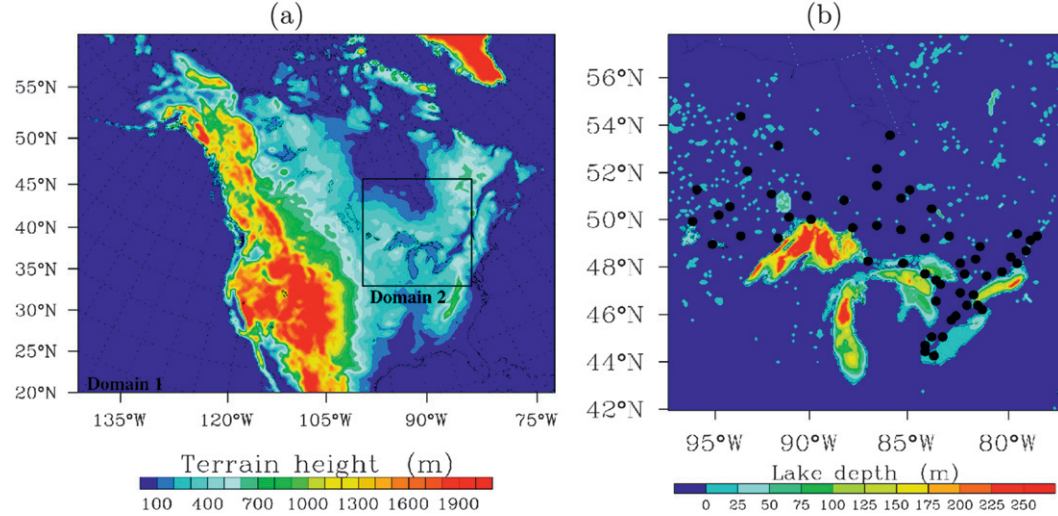


FIG. 1. (a) The map of North America showing the WRF 30-km horizontal resolution domain over North America (domain 1) and the 10-km horizontal resolution domain over Ontario and the Great Lake Basin (domain 2). (b) Lake depth for the Ontario and Great Lake Basin from the global lake dataset (Kourzeneva 2009). Black dots in (b) show the spatial distribution of the Canadian rehabilitated precipitation dataset stations.

the coupling among the earth's atmosphere, oceans, land surface, and sea ice, which are individual modules that interact with one another via a central coupler component. We employ the version of the model at T85 resolution for the atmosphere and land, which operates on a 256×128 regular longitude-latitude global horizontal grid (giving a 1.4° resolution) with 26 levels in the vertical. Output from an experiment run with observed twentieth-century greenhouse gases was used to force the historical WRF simulations. The global simulation used in this study for future climate projection was forced with the Special Report on Emissions Scenarios (SRES) A2 emissions scenario (Nakicenovic and Swart 2000). The A2 scenario assumes a relatively aggressive “business as usual” increase in atmospheric carbon dioxide emissions over the twenty-first century.

b. The regional climate model: WRF

The regional meteorological model being employed in this ongoing project is the Weather Research and Forecasting (WRF) model with the Advanced Research WRF (ARW) dynamic core, version 3.2.1 (Skamarock et al. 2007). WRF is a next-generation, limited area, nonhydrostatic model, with a terrain-following eta-coordinate mesoscale modeling system designed to serve both operational forecasting and atmospheric research needs. We choose WRF because it is being developed and studied by a broad community of government and university researchers. The simulations to be discussed herein have been performed with the 3.2.1 version of the model with the following physical options: the WRF

single-moment 6-class (WSM6) microphysical parameterization (Hong et al. 2004); the Community Atmosphere Model, version 3 (CAM3) shortwave and longwave radiation scheme, similar to the scheme used in CCSM, which allows for aerosols and trace gases; the Yonsei University (YSU) planetary boundary layer (PBL) scheme (Noh et al. 2003), and the Noah land surface model (Chen and Dudhia 2001).

Additional options from the version of WRF intended for climate applications (Fita et al. 2009) have also been incorporated in the 3.2.1 version. One of the main capabilities added to the model is that which enables the output of mean and extreme statistics of surface variables at every time step, making model output much more comparable to observational data. Another added capability is the ability to assimilate and update variable mixing ratios for the radiatively active trace gases CO₂, N₂O, CH₄, chlorofluorocarbon (CFC)-11, and CFC-12 during the simulation. The concentration of these gases prescribed in the WRF simulations that we will describe were chosen to be identical to those in the corresponding parent CCSM simulation.

The spatial setup of WRF is composed of two domains, a 30-km parent domain covering the whole of Canada and most of North America and a 10-km one-way nested domain covering the Canadian province of Ontario and the Great Lakes Basin (Fig. 1). The model outer domain is centered at 50°N, 100°W with dimensions of 290×200 horizontal grid points. The Lambert conformal conic projection is used as the model horizontal coordinates with the standard parallel at 50°N. In the vertical, we use 28 terrain-following eta levels.

Initial and boundary conditions for the large-scale atmospheric fields, as well as sea ice and sea surface temperature (SST), are obtained from the CCSM model output. The domain specified lateral boundary is composed of a 1-point specified zone and a 9-point relaxation zone. Boundary conditions at the specified zone are determined entirely by temporal interpolation from the 6-hourly CCSM data. Lateral boundary conditions at the relaxation zone are nudged toward the forcing data following the method of Davies and Turner (1977), with higher nudging coefficients for grid points that are closer to the specified zone. The SST, sea ice, and green vegetation fraction are also updated every 6 h during the simulations.

Spectral nudging is included in WRF 3.2.1 to prevent synoptic-scale climate drift generated by the formulation of lateral boundary conditions over an open system during long-term simulations (Miguez-Macho et al. 2004). Simulations were run using spectral nudging at all levels above the planetary boundary layer, unless the latter is below grid level 8 (about 1000 m). The spectral nudging employed is reasonably weak, used for wavelengths longer than ~ 2000 km and applied for temperature and horizontal winds in the outer domain only. Moisture is not nudged at any level. Thus, this approach maintains the objective of downscaling, which is to generate mesoscale meteorological details consistent with the large-scale state simulated by the global model.

c. Derivation of lake surface data

Since the WRF model does not currently have a sufficiently detailed explicit lake component, lake water temperature needs to be prescribed externally in the model as well as SST. Heat and water fluxes between the lake surface and the atmosphere are then computed within the WRF model at each time step using the provided lake water temperature.

The CCSM model accounts for the presence of inland water bodies such as the Great Lakes through the use of a 1D lake model included in the CLM land component. The formulation of the lake model (Zheng et al. 2002) is based on the coupled lake–atmosphere model of Hostetler et al. (1993, 1994) and simulates temperatures for 10 layers with a fixed 50-m lake depth. However, the resolution of the CCSM model is too coarse to produce accurate lake ice cover and lake surface water temperature for high-resolution regional simulations.

As a preliminary step en route to the development of a new version of WRF that is fully coupled to an appropriate lake model, in the analyses to be described in what follows we present results based upon offline coupling of the freshwater model FLake forced by the meteorological fields from the CCSM simulation to provide the lake

water temperature and lake ice evolution for use in the regional climate simulations.

Computationally efficient 1D lake models, which range from one-layer bulk models to multilayer turbulence closer models [see Mironov (2008) and references therein], have been developed to be used as the basis for GCM and RCM parameterization schemes. To be coupled with an atmospheric model, a lake model needs to be computationally inexpensive, should incorporate most of the essential physics, should not require tuning for a particular lake, and should require a minimum set of specific lake parameters. All of these restrictions are important and are met by the FLake model (Mironov 2008), which has already been incorporated in different atmospheric models such as the numerical weather prediction model of the Consortium for Small-Scale Modeling (COSMO; Mironov et al. 2010). Performance assessment of the model in the Great Lakes region has shown that despite its relative simplicity the FLake model performed well with respect to lake surface temperature and to the timing of freeze-up and ice break-up (Martynov et al. 2010).

The FLake model is based on a two-layer parametric representation of the evolving temperature profile, with a mixed layer at the surface and a thermocline extending from the bottom of the mixed layer to the bottom of the lake [see Mironov (2008) for a detailed description of the model]. The lake thermocline is described using the concept of self-similarity of the thermal structure of the water column, which originates from observations of oceanic mixed layer dynamics (Kitaigorodskii and Miropolsky 1970). The same parametric concept is applied to the temperature structure of the bottom sediment layer and of the ice and snow layers. A system of prognostic ordinary differential equations is solved for the time-dependent quantities, which are the mixed layer temperature and depth, the lake ice thickness and temperature, and the temperature and depth of the layer of bottom sediments penetrated by the annual thermal wave. Convective entrainment, wind-driven mixing, and volumetric solar radiation absorption are included in the formulation of the mixed layer depth equation.

The main external parameter for the FLake model is the lake depth, since this will determine the amount of heat it is capable of storing and hence the time needed for the lake to cool and ultimately freeze at the surface. For the purpose of the following analyses we have employed data from the Global Lakes Dataset (Kourzeneva 2009) in the two WRF domains. Lake depths for Ontario and the Great Lakes Basin at 10-km resolution are also shown in Fig. 1.

The two-layer water temperature parameterization, however, limits the ability of the FLake model to simulate

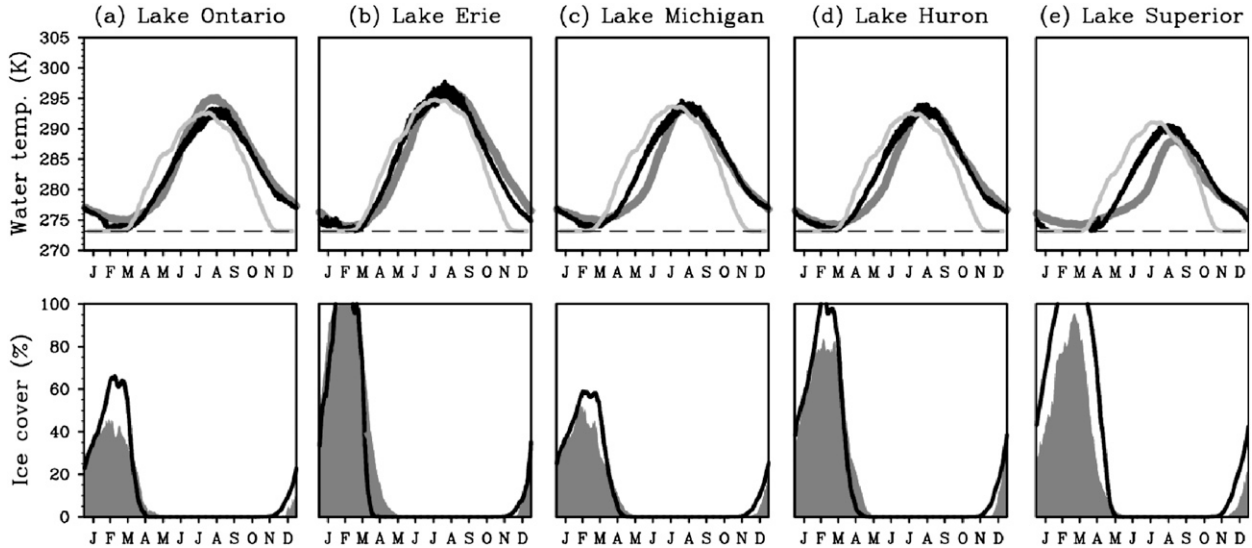


FIG. 2. (a)–(e) Lake surface water temperature (K) and ice cover (%) averaged over each of the five Great Lakes for the 1981–2001 period as simulated by FLake forced by atmospheric conditions derived from the global CCSM model (black) and observations (dark gray). The light gray line corresponds to a 1-week running average of the surface temperature as simulated by CCSM averaged over each of the five Great Lakes.

very deep lakes, and in such cases it is suggested by model developers that a “virtual bottom” at 60-m depth with the bottom-sediment module switched off be employed instead of actual lake depth. Because the deep abyssal zones typically experience no appreciable temperature changes, when using this false bottom approximation one can expect FLake to produce satisfactory results.

In summary, two WRF simulations were run for historical (1979–2001) and future (2050–60) conditions as two continuous runs with a 1-yr equilibration. Lateral boundary conditions for the outer domain at 30-km resolution are provided by the global CCSM simulation. The inner nested domain is driven using lateral boundary conditions from the coarser WRF domain only. Lake surface temperature and ice cover prescribed in the WRF simulations are derived from the CCSM-driven FLake simulations for both domains.

3. Model evaluation

a. Evaluation of the CCSM-FLake results for the modern instrumental era

To provide the lake surface data for the regional WRF simulations, the lake model FLake was applied throughout the two model domains shown in Fig. 1. The following meteorological fields from the CCSM simulation, interpolated on the 30- and 10-km grids, were employed to force the model with a 6-h time step: air temperature, pressure, humidity, wind components (all at 2-m height), and downward shortwave and longwave radiation fluxes

at the surface. A 23-yr (1979–2001) simulation of water and ice evolution was performed, preceded by a 10-yr spinup to ensure no dependence on the prescribed initial state.

For validation of model results, we have employed the following datasets:

- 1) Lake surface temperature from the Advanced Very High Resolution Radiometer (AVHRR) produced by the Group for High-Resolution Sea Surface Temperature (GHRSST) at NOAA’s National Climatic Data Center (NCDC), as described in Reynolds et al. (2007), and which extends back to September 1981. This analysis is produced daily at 0.25° resolution from satellite data with a bias correction using in situ data from ships and buoys.
- 2) Ice observations from the Great Lakes Ice Atlas (Assel 2003) produced by the Great Lakes Environmental Research Laboratory (GLERL) at the National Oceanic and Atmospheric Administration (NOAA), which provide daily ice concentrations over the Great Lakes for the winter seasons on a nominal spatial resolution of 2.5 km.

Figure 2 shows the simulated surface water temperature and ice cover averaged over each of the five Great Lakes in comparison with AVHRR observations and ice observations from GLERL for the period 1981–2001. The lake temperatures simulated by CCSM show a similar behavior for all lakes with an early and synchronized warming in early spring and a rapid cooling in late autumn, following closely the large-scale seasonal cycle of

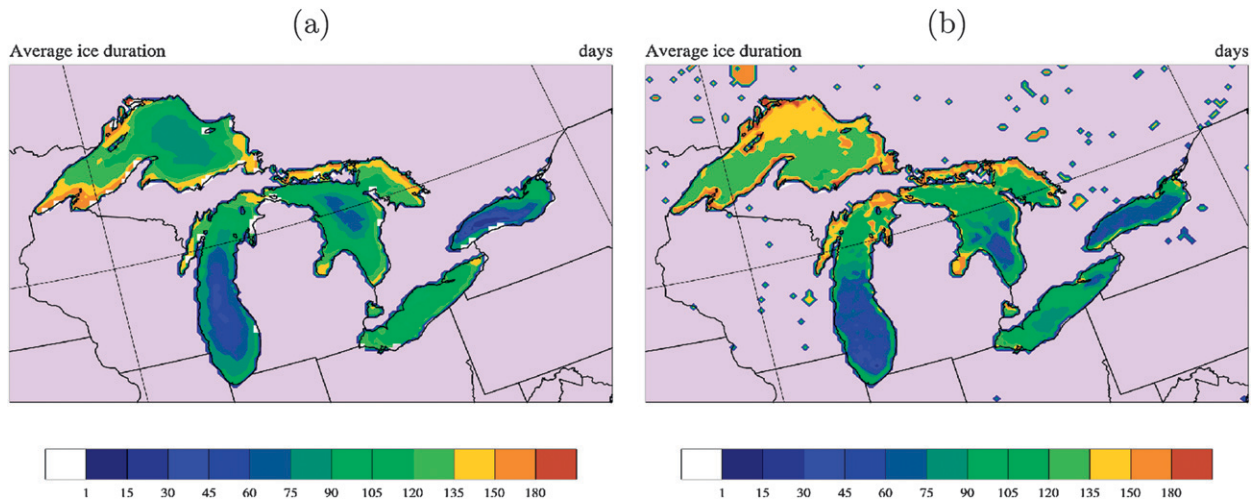


FIG. 3. Average ice duration in days for the Great Lakes, (a) observed for the 1979–2001 historical period and (b) simulated by FLake driven by CCSM atmospheric fields for the 1979–2001 historical period.

air temperature. Comparison with observation shows large differences during these periods, increasing with the depth of the lakes. While the temperature evolution of the small and shallow lakes follows closely the atmospheric conditions, a large temporal lag in energy and water cycling is observed for large and deep lakes due to their considerable heat storage capacity. These biases are partially corrected in the FLake output, which produces delayed warming and cooling of the lakes. Lake temperatures are in very good agreement during the cooling phase of the lakes, from midsummer to late winter, except for a small cold bias for Lake Erie. The distinction between the spring warming patterns is also greatly reduced, but is still present for the three deepest lakes and particularly for Lake Superior. This discrepancy can be partially attributed to the use of CCSM meteorological fields, which underestimate the influence of the Great Lakes, as the driving data for the lake model. Similar biases have been observed in previous studies (Martynov et al. 2010) where 40-yr European Centre for Medium-Range Weather Forecasts (ECMWF) Re-Analysis (ERA-40) data were used to drive the FLake model over the Great Lakes.

This characteristic pattern captured by observations in very large lakes, with a slow and prolonged warming of the surface water from 0° to 4°C , reflects the presence of a deep convective mixed layer during this period, typical for central parts of large deep freezing lakes (Beletsky and Schwab 2001). During the process of lake stratification, shallow areas generally become stratified before deeper areas. In large lakes this condition may persist for weeks, during which a temperature front known as a thermal bar forms between the stratified and

unstratified areas of the lake (Assel 1986; Boyce et al. 1989). As stated by Martynov et al. (2010), the lack of representation of horizontal mass and heat transfer in 1D lake models, as well as other nonlocal physical phenomena, may contribute to the differences between model simulations and observations.

Comparisons of simulated (black line) and observed ice cover (dark gray line) are shown in Fig. 2. The ice freeze-up and break-up dates appear to be in quite reasonable agreement with the observations from GLERL. However, illustrations of the previously discussed limitations related to the biases in the atmospheric forcings and 3D effects in the large and deep lakes are seen for Lake Erie and Lake Superior, respectively. The too early ice break-up in spring observed for Lake Erie, which is the most sensitive to atmospheric variations because of its shallowness, directly follows biases in the CCSM driving simulation. The ice concentration is also a bit overpredicted for Lake Superior because of the difficulty of the lake model in reproducing temperature and ice variations in the deep central part of the lake. Observed and model-simulated average ice durations for the Great Lakes for the period 1979–2001 are shown in Figs. 3a and 3b, respectively. The simulated ice cover period is in good agreement with observations for most parts of the lakes. The main differences are seen in the deepest parts (depth >200 m; see Fig. 1b) of Lake Superior and Lake Michigan. As was the case for temperature, the model is fairly successful in reproducing the observed spatial patterns and the rather substantial differences from one lake to the next and provides a great improvement compared to the original CCSM simulated lake temperature and ice cover.

b. Evaluation of the WRF downscaled results

To evaluate the performance of the WRF-based regional climate model downscaling methodology, we compare the results from a 23-yr simulation of the present climate from the driving model CCSM and from the WRF-based downscaling results with the observed data for surface climate. The lake water temperatures from the FLake simulation described previously are prescribed in the WRF simulation. Comparisons focus on mean (T_{mean}), daily maximum (T_{max}), daily minimum (T_{min}) temperatures and precipitation in the inner domain. As the CCSM model does not have a direct time correspondence with observations, we focus in the following on comparisons of annual and seasonal cycles averaged over the 1979–2001 historical period.

1) OBSERVATIONAL AND REANALYSIS DATA

We have employed several different datasets in evaluation of the surface climate fields produced by the CCSM model and further downscaled with the WRF model. These datasets include the following:

- 1) The North American Regional Reanalysis (NARR) data are from the 32-km National Centers for Environmental Prediction (NCEP) NARR dataset. The quality of NARR data has been evaluated with surface station and sounding measurements (Mesinger 2006). Hence, it has been used in numerous studies for validation of regional climate simulations in North America (e.g., Lo et al. 2008).
- 2) The Climatic Research Unit (CRU) observational data are a high-resolution ($0.5^\circ \times 0.5^\circ$) gridded dataset of monthly-mean surface climate over global land areas (New et al. 2002; Mitchell and Jones 2005), version 3.0 of which (CRU TS3.0, 2008) is available through the Climatic Research Unit at the University of East Anglia. These gridded data are based on an archive of monthly mean, maximum, and minimum temperature and precipitation data provided by more than 4000 weather stations distributed globally.
- 3) The Global Precipitation Climatology Centre (GPCC) observational data are another high-resolution ($0.5^\circ \times 0.5^\circ$) gridded dataset of monthly-mean precipitation over the globe. They are available through the Global Precipitation Climatology Centre (Rudolf et al. 2005).
- 4) The Canadian Rehabilitated Precipitation Dataset (CRPD) from the National Climate Data Archive of Environment Canada, which consists of monthly totals of daily rainfall, snowfall and total precipitation for more than 400 locations across Canada (Mekis and Hogg 1999). Details of adjustment methodology and corrections applied to the data are described in Devine and Mekis (2008) and Vincent and Mekis

TABLE 1. Regression analysis of the historical WRF and CCSM simulated mean, maximum, and minimum temperature over Ontario and CRU observations.

	WRF			CCSM		
	Corr	Slope	RMSE	Corr	Slope	RMSE
Annual temp (K)	0.99	1.08	0.63	0.99	1.12	0.87
Winter temp (K)	0.99	0.99	0.77	0.99	0.91	1.04
Summer temp (K)	0.97	1.25	0.98	0.96	1.60	1.94
Annual T_{max} (K)	0.99	1.09	0.74	0.98	1.24	1.31
Winter T_{max} (K)	0.99	0.96	0.73	0.98	0.86	1.10
Summer T_{max} (K)	0.97	1.32	1.26	0.95	2.03	3.11
Annual T_{min} (K)	0.98	1.05	0.86	0.98	1.03	0.87
Winter T_{min} (K)	0.98	1.01	1.20	0.98	0.95	1.23
Summer T_{min} (K)	0.94	1.09	1.04	0.92	1.15	1.23

(2009). The spatial distribution of these stations is shown in Fig. 1.

2) TEMPERATURE

Table 1 shows the results of a regression analysis of annual and seasonal simulated T_{mean} , T_{max} , and T_{min} for the forcing CCSM and the WRF simulation, compared to the CRU grid observations averaged over the 1979–2001 period. For both models, the annual T_{mean} , T_{max} , and T_{min} show a very high spatial correlation with a regression coefficient (slope) close to 1 (see Table 1). The root-mean-square error (RMSE) is reduced in the WRF simulation, especially for T_{max} , which has the lowest accuracy in the CCSM simulation. The winter season is characterized by similar skill (as is the case in spring and fall; not shown). A noticeable bias is observed in the summer season (June–August) where the WRF simulation has a cold bias in T_{mean} and T_{max} , which is directly inherited from an even stronger bias in the forcing CCSM data. The large RMSE for T_{mean} and T_{max} simulated by CCSM during summer is greatly reduced in the WRF simulation.

Annual, winter, and summer T_{mean} biases of the driving CCSM model and WRF compared to NARR reanalysis for the historical period (1979–2001) are shown in Fig. 4. The annual mean temperature over the domain for the CCSM simulation (Fig. 4a) is quite reasonable compared to the results from the NARR reanalysis. The main differences are seen in the vicinity of the Great Lakes and north of the domain, close to Hudson Bay. The moderating effect of the Great Lakes on temperature is not well reproduced. Temperatures are too warm in summer and too cold in winter with the greatest variations over Lake Superior, with a bias of up to -5°C in winter and $+3^\circ\text{C}$ in summer (Figs. 4b,c). A strong cold bias is also seen in summer around Hudson Bay. These biases are greatly attenuated in the downscaled WRF

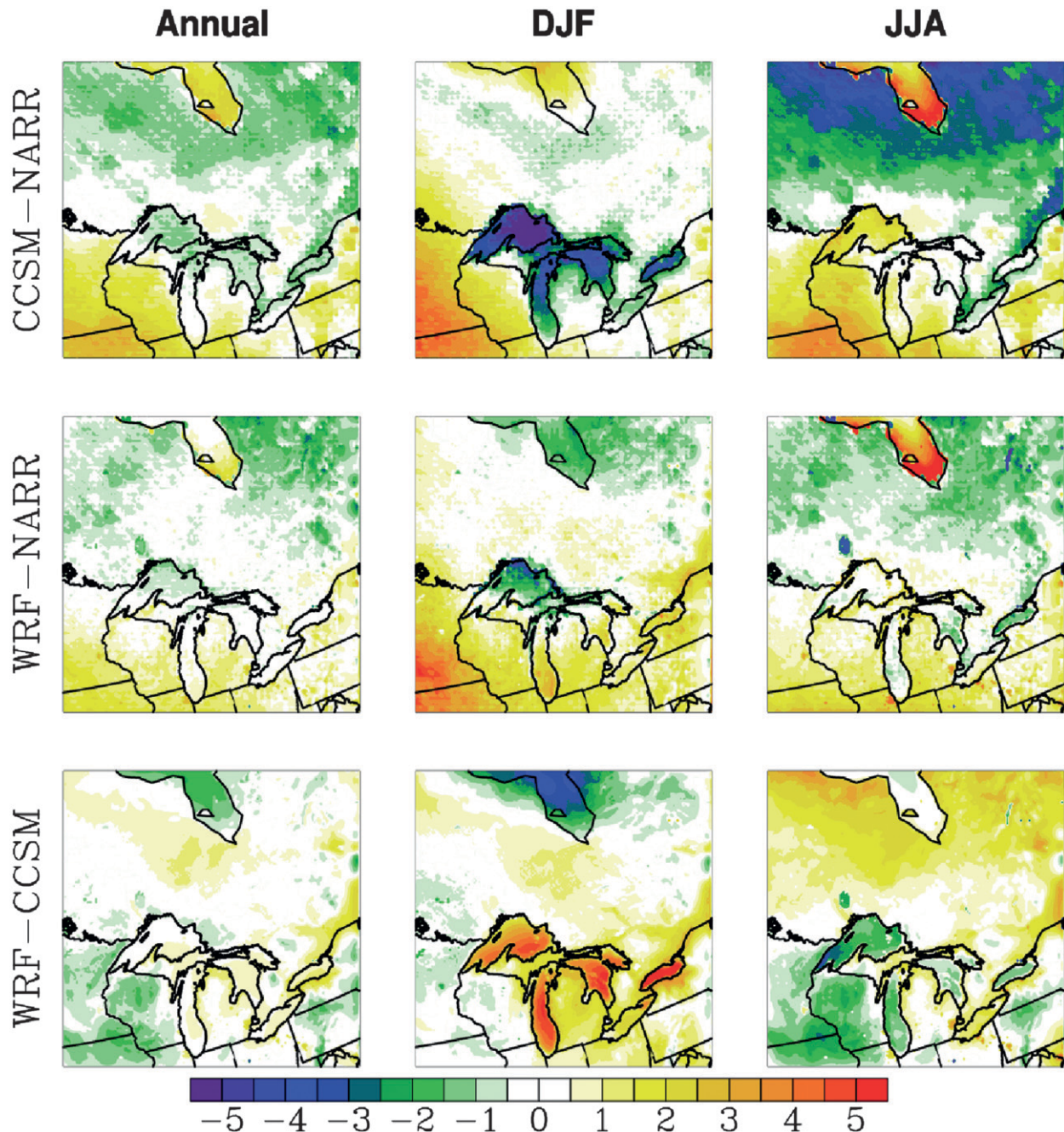


FIG. 4. The surface 2-m air temperature (K) biases (from NARR reanalysis) of the driving (top) CCSM and (middle) WRF, and (bottom) differences due to the downscaling. Shown are annual, winter, and summer averages for the historical period (1979–2001).

simulations (Figs. 4d–f) with a much more realistic seasonal temperature cycle in the Great Lakes region.

3) PRECIPITATION

Figure 5 shows the spatial patterns for total precipitation from the forcing CCSM data and WRF simulation for the historical period. These fields are to be compared with the two different sets of observations,

namely, the GPCC and CRU observational datasets. The large-scale fields from the CCSM simulation (Figs. 5a–c) are quite reasonable in winter, except that they are, as expected, unable to reproduce small-scale structures, but they behave very poorly in the summer season with a large underprediction of precipitation. These deficiencies are corrected in the WRF simulations with a highly significant improvement in the summer season.

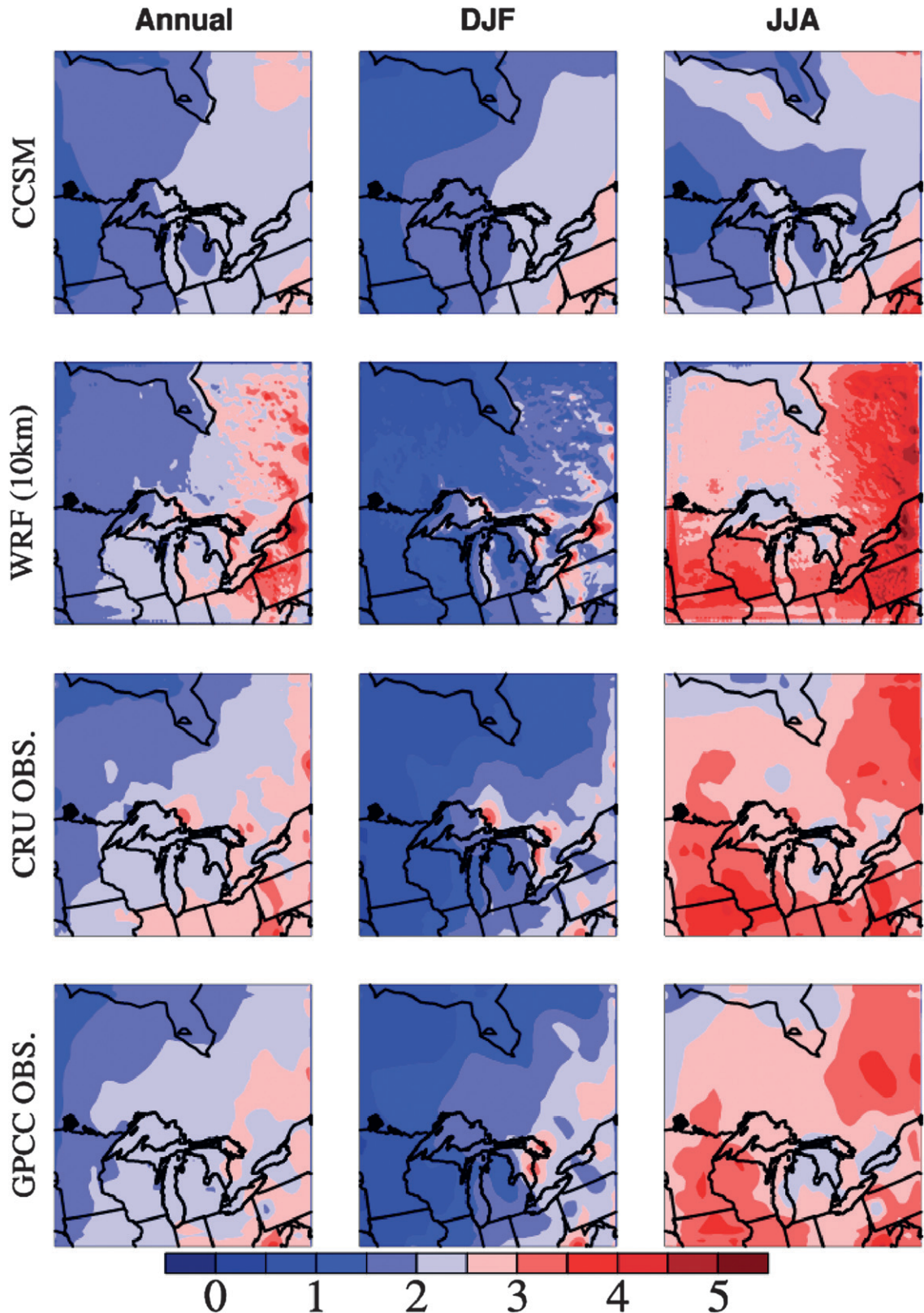


FIG. 5. Annual, winter, and summer precipitation (mm day^{-1}) for the historical period (1979–2001) from (first row) CCSM, (second row) WRF, (third row) CRU observations, and (fourth row) GPCC observations.

TABLE 2. Regression analysis of the historical WRF and CCSM simulated precipitation over Ontario and CRU observations.

	WRF			CCSM		
	Corr	Slope	RMSE	Corr	Slope	RMSE
Annual precipitation (mm day^{-1})	0.77	1.07	0.30	0.66	0.60	0.28
Winter precipitation (mm day^{-1})	0.80	0.92	0.34	0.80	0.60	0.33
Summer precipitation (mm day^{-1})	0.58	0.83	0.43	-0.21	-0.17	0.54
Jan precipitation (mm day^{-1})	0.80	0.86	0.36	0.80	0.52	0.48
Feb precipitation (mm day^{-1})	0.81	1.03	0.37	0.81	0.73	0.65
Mar precipitation (mm day^{-1})	0.83	0.96	0.43	0.83	0.93	0.66
Apr precipitation (mm day^{-1})	0.78	0.78	0.53	0.61	0.45	0.66
May precipitation (mm day^{-1})	0.77	0.98	0.75	0.04	0.02	0.62
Jun precipitation (mm day^{-1})	0.74	1.26	0.63	-0.12	-0.08	0.90
Jul precipitation (mm day^{-1})	0.32	0.46	0.68	-0.16	-0.12	1.05
Aug precipitation (mm day^{-1})	0.27	0.34	0.55	-0.17	-0.17	1.06
Sep precipitation (mm day^{-1})	0.69	1.16	0.68	0.52	0.60	1.70
Oct precipitation (mm day^{-1})	0.66	0.90	0.59	0.45	0.39	0.66
Nov precipitation (mm day^{-1})	0.72	0.92	0.53	0.70	0.65	0.45
Dec precipitation (mm day^{-1})	0.75	0.87	0.43	0.72	0.51	0.56

Nevertheless, the precipitation is slightly overpredicted compared to observations in the eastern part of the domain. The precipitation produced by the grid-scale convection (which is predominant in the winter season) is in very good agreement with the observations in terms of amplitudes and spatial pattern at all times. The difficulty arises from the part of the precipitation due to the cumulus parameterization that is predominant in the summer season, which is overpredicted in the WRF simulations, especially in the Quebec region. One of the reasons for this may be the poor modeling of SST in the Gulf Stream region in the CCSM model (and the majority of GCMs; e.g., Bukovsky and Karoly 2008), which induces large uncertainties for the prediction of precipitation over the east coast of Canada. This effect is inherited from the forcing at the eastern boundary of the domain by the CCSM data. A clear improvement is also seen in the winter season as the WRF simulations are able to recover the finescale patterns due mainly to the presence of the Great Lakes. The lake effect is quite visible in the winter season (Fig. 5e) with localized increases of precipitation in the downwind regions of the lakes.

Results of regression analysis of mean annual, seasonal, and monthly precipitation averaged over the 1979–2001 period for the WRF and CCSM simulations compared to the CRU grid observations are presented in Table 2. Results for precipitation are not characterized by the same skill as found for temperature but are nevertheless in reasonable agreement with observations. Spatial correlations for the WRF simulation are especially good from November to March in the cold season, but they revert to reduced skill in the spring and summer seasons. Precipitation is slightly overpredicted, especially between May and July. The results are in any

event greatly improved compared to the globally underpredicted precipitation in the forcing CCSM data, which show reasonable agreement in the cold season but very poor skill in summer. The spatial patterns of correlation, RMSE, and bias for the monthly averaged precipitation are plotted in Fig. 6. As seen from the low correlation coefficients and large RMSE, the CCSM model does not capture the annual cycle of precipitation well in the vicinity of the Great Lakes. Strong negative biases are also seen downwind of the lakes because of the limitations of the CCSM model in the simulation of small-scale lake–atmosphere interactions responsible for the lake-induced precipitation. The annual cycle of precipitation is greatly improved in the WRF simulation with a higher correlation throughout the domain, smaller RMSE, and a reduced bias in most parts of the domain, except for the positive bias seen in the easternmost region.

A closer look at the distribution of mean annual snowfall in the Great Lakes Basin is displayed in Fig. 7 for CCSM and WRF. The domain averaged amount of snowfall is quite comparable for both models but the spatial distribution reveals extreme differences. The CCSM simulation shows no impact of the lakes on the snowfall distribution, and a quasi-zonal distribution is observed. On the other hand, the WRF simulation displays very large contrasts in the vicinity of the Great Lakes. Local maxima of snowfall due to the lake-effect snow are observed downwind of the lakes, in the areas referred to as snowbelts. The simulation clearly identifies seven of these associated with the five Great Lakes, namely, 1) the southeastern Lake Ontario snowbelt, centered on Tug Hill Plateau immediately east of Lake Ontario in upstate New York; 2) the southeastern Lake Erie snowbelt

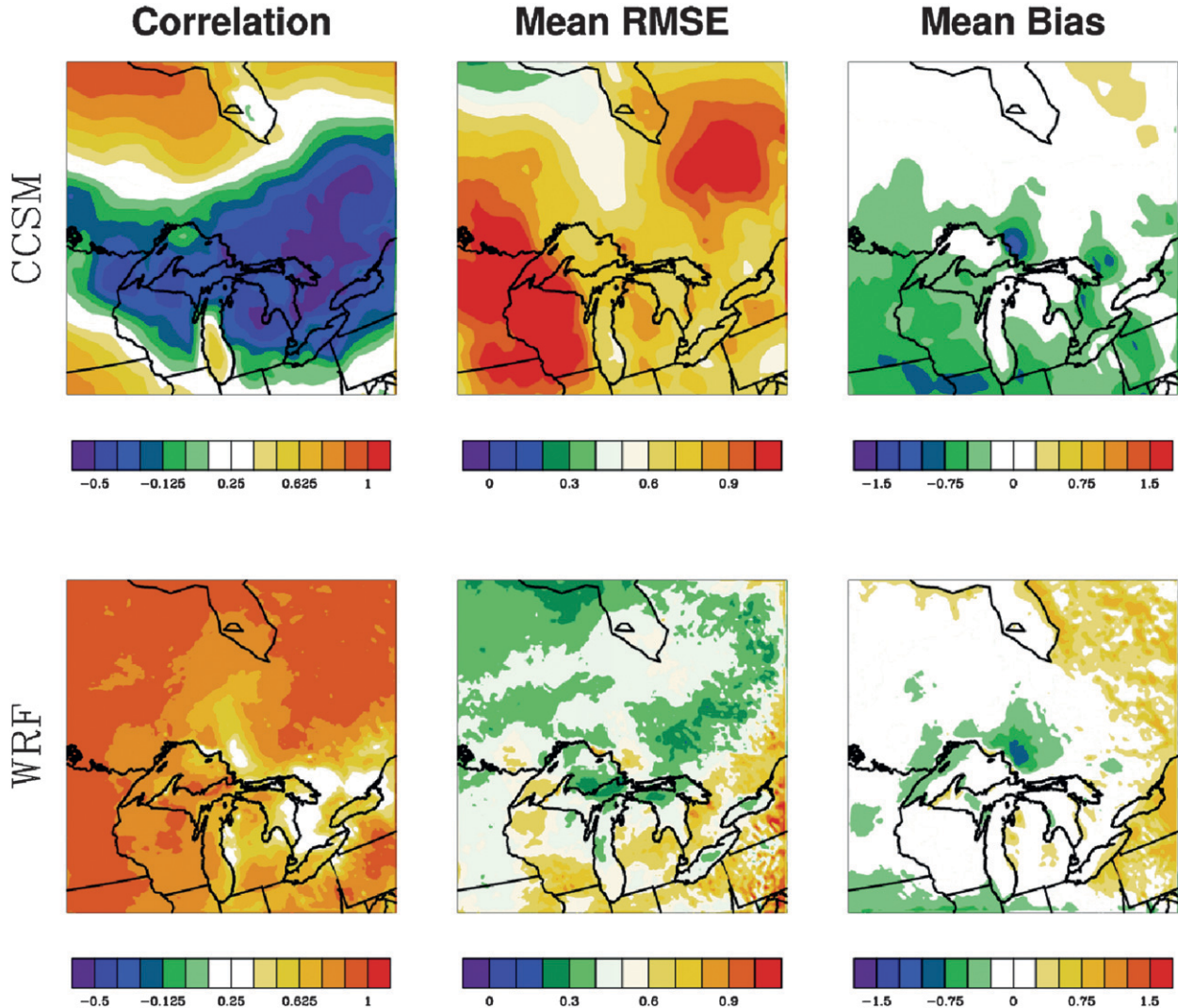


FIG. 6. Maps showing correlation, RMSE and bias computed for monthly averaged precipitation (mm day^{-1}) for the historical period (1979–2001) from the (top) CCSM and (bottom) WRF simulations compared to CRU observations.

in the uplands of the Allegheny Plateau back from the lake front in New York, Pennsylvania, and northeastern Ohio; 3) the southeastern Lake Huron snowbelt in southwestern Ontario; 4) the Georgian Bay snowbelt along the eastern shore of Georgian Bay in central Ontario; 5) the eastern Lake Michigan snowbelt, covering the western shore of the state of Michigan and the northern shore of Indiana; 6) the eastern Lake Superior snowbelt; and 7) the southeastern Lake Superior snowbelt. Results of regression analysis of annual simulated and observed total precipitation and snowfall for the WRF and CCSM simulations compared to the Canadian rehabilitated precipitation dataset at the stations plotted in Fig. 7 for the 1979–2001 period are presented in Table 3. The 35 stations situated in the Great Lakes Basin (domain of Fig. 7) have been

considered. Stations showing a mean annual snowfall greater than 250 mm water equivalent (mm w.e.) are plotted as white filled dots. Precipitation is still underpredicted in the CCSM simulation, due mainly to the strong bias in the summer period, but snowfall appears to be in more reasonable agreement with observations. The main problem, as seen previously, is the absence of the lake effect, which leads to a large underprediction of snowfall in the snowbelt areas. Precipitation and snowfall show a better agreement for the WRF simulation. Snowfall is also underpredicted in the WRF simulation compared to observations but the spatial correlation is greatly improved. A much better agreement is observed for stations situated in the snowbelts, which are characterized by the greatest snowfall in both observations and the WRF simulation.

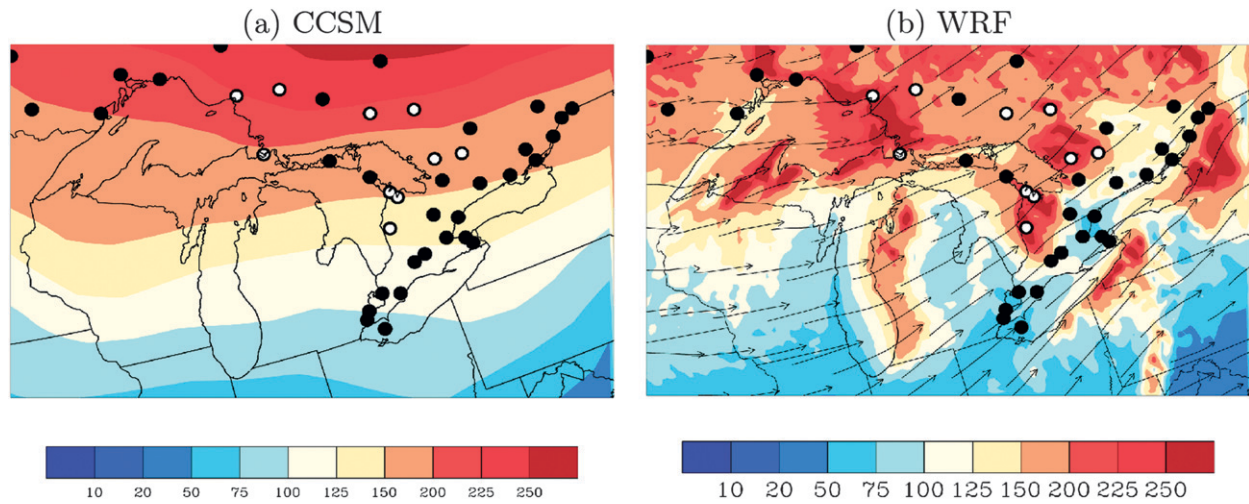


FIG. 7. Contours of mean annual snowfall [water equivalent mm (mm w.e.)] for the historical period (1979–2001) from (a) CCSM and (b) WRF. Vectors in (b) show the mean surface velocity field during the fall and winter season from the WRF simulation. The black dots show the spatial distribution of the Canadian rehabilitated precipitation dataset stations. Stations showing a mean annual snowfall greater than 250 mm w.e. correspond to white filled dots.

4. The impact of global warming on the Great Lakes Basin

Changes in the seasonal and annual means and annual cycle of temperature and precipitation from the historical period to the middle of the twenty-first century are presented in this section.

a. Lake ice and temperature for the mid-twenty-first-century future scenario

The FLake simulation, driven by CCSM atmospheric fields, was continued for the 2001–2100 period under the IPCC SRES A2 scenario. Evolution of surface air and lake water temperatures and corresponding ice cover are plotted in Fig. 8. Following the warming of air temperature predicted by the CCSM simulations, the surface lake temperature rises and the percent of ice cover is greatly diminished. Figure 9 shows the changes in lake water temperature and ice duration for the 2050–60 period compared to the historical period. The fall and spring season air temperature warming of $\sim 2^{\circ}$ to 4°C translates into a reduction in lake ice cover period on the order of 25 days for the shallow Lake Erie, 30 days for Lake

Ontario, 35 days for Lake Huron, 40 days for Lake Michigan, and up to 50 days for Lake Superior. An earlier break-up (15–20 days), strongly related to the shift in air temperature, is observed for all locations. All locations also exhibit a later freeze-up, but the amplitude of the shift is quite variable (3 to 20 days) depending on the location.

b. Projected temperature changes

To understand the impact of these changes in lake temperature and ice cover, the WRF simulation was performed using these outputs from the FLake model driven by the CCSM outputs for the future period.

Changes of the mean temperature in the whole domain are shown in Fig. 10. The spatial pattern and the magnitude of the projected temperature change are quite similar for both models. These changes exhibit strong spatial gradients as a change of 2.0° – 3.0°C is observed in southern Ontario but this increases to 3.0° – 4.0°C in northern Ontario, with the greatest warming occurring in the Hudson Bay region. In winter, the largest projected changes are in the northern part of

TABLE 3. Regression analysis of the historical CCSM and WRF simulated annual total precipitation (mm) and annual snowfall (mm w.e.) vs all station observations and vs station observations situated in the snowbelts only (see Fig. 7).

	Stations	WRF				CCSM		
		Corr	Slope	RMS	Bias	Corr	Slope	RMS
Precipitation (mm)	All	0.85	1.12	105	-66.5	0.59	0.39	212.6
Precipitation (mm)	Snowbelts	0.91	1.24	116.8	-86.4	0.51	0.13	327.7
Snowfall (cm)	All	0.86	0.80	53.7	-36.4	0.69	0.38	80.0
Snowfall (cm)	Snowbelts	0.63	1.04	54.7	-41.4	-0.10	-0.20	150.2

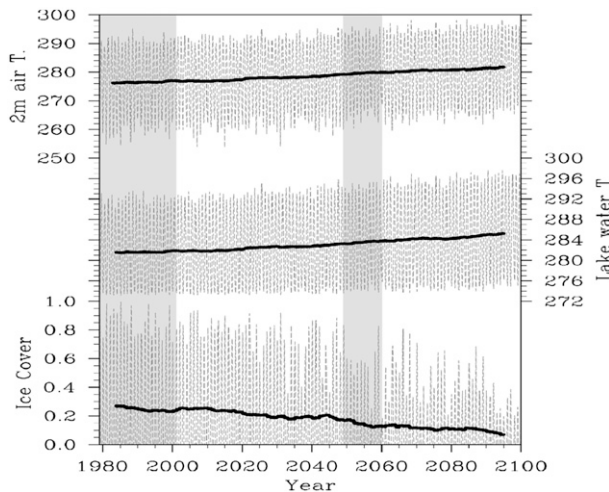


FIG. 8. (top) The 2-m air temperature (K) from CCSM under the A2 scenario averaged over Ontario and the Great Lakes Basin (Fig. 1b), (middle) lake water temperature (K), and (bottom) ratio of ice-covered lake surface by total lake area from the FLake simulation averaged over the five Great Lakes. Dashed black lines correspond to monthly mean and thick black lines to 10-yr running averages.

Ontario, with changes as large as 5°C in the Hudson Bay region and in the vicinity of Lake Superior and $3^{\circ}\text{--}4^{\circ}\text{C}$ in the northern part of Lake Michigan and Lake Huron. The projected summertime temperatures are far more modest, with the southern part of Ontario experiencing the largest changes (on the order of $2^{\circ}\text{--}3^{\circ}\text{C}$). The main differences between the WRF and CCSM simulations are clearly located in the vicinity of the Great Lakes. A larger temperature change is seen for Lake Superior and the northern parts of Lake Huron and Lake Michigan in the WRF simulation compared to the CCSM simulation. In these areas where the decline in ice cover is the most

significant (Fig. 9), the longer ice-free period amplifies the warming effect of the lakes on the atmosphere and increases temperature in excess of the regional atmospheric warming. The earlier break-up of ice causes the onset of the positively stratified season to occur earlier, leading to a stronger trend in mean summer temperature as well, as was observed in other recent studies (Austin and Colman 2007) for the historical period.

c. Projected precipitation changes

Precipitation rate and intensity can change because of a large number of processes, including changes in water vapor content of the atmosphere, changes in cloud cover and type, and atmospheric lapse rates and stability profiles (Trenberth et al. 2003). In general, most of North America is projected to see an increase in precipitation under increasing greenhouse gas concentrations. Results from the IPCC AR4 climate simulations indicate that as surface temperature increases, total atmospheric water vapor increases and precipitation increases by roughly $2.2\% \text{ K}^{-1}$ (Held and Soden 2006). However, precipitation changes are highly nonuniform spatially and do not display a simple relationship with water vapor change. Both for CCSM and WRF downscaled results, the amount of annual mean precipitation is projected to show a significant increase over most of Canada, Alaska, and the eastern seaboard (not shown). However, precipitation changes are projected to be far smaller over most of the interior of the landmass, and results from various models under different scenarios show the greatest uncertainty in regions such as the Great Lakes Basin.

Precipitation changes for the 2050–60 period compared to 1979–2001 are shown in Fig. 11 for the CCSM and WRF simulations. Compared to the globally increasing precipitation in the CCSM simulations, which

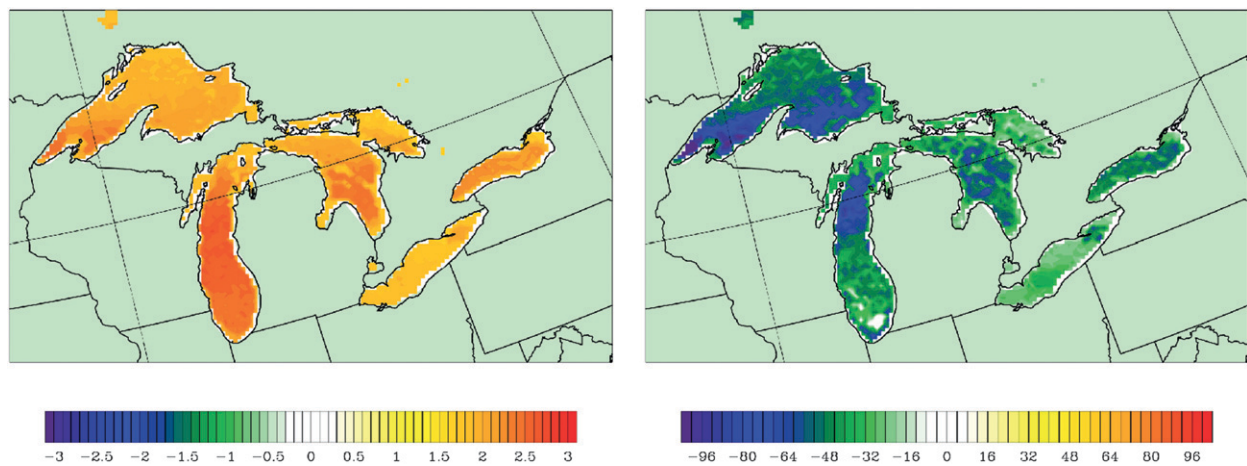


FIG. 9. Changes in (left) lake water temperature (K) and (right) ice duration (days) for the Great Lakes simulated by FLake driven by CCSM atmospheric fields for the 2050–60 period following scenario SRES-A2 compared to the historical period 1979–2001.

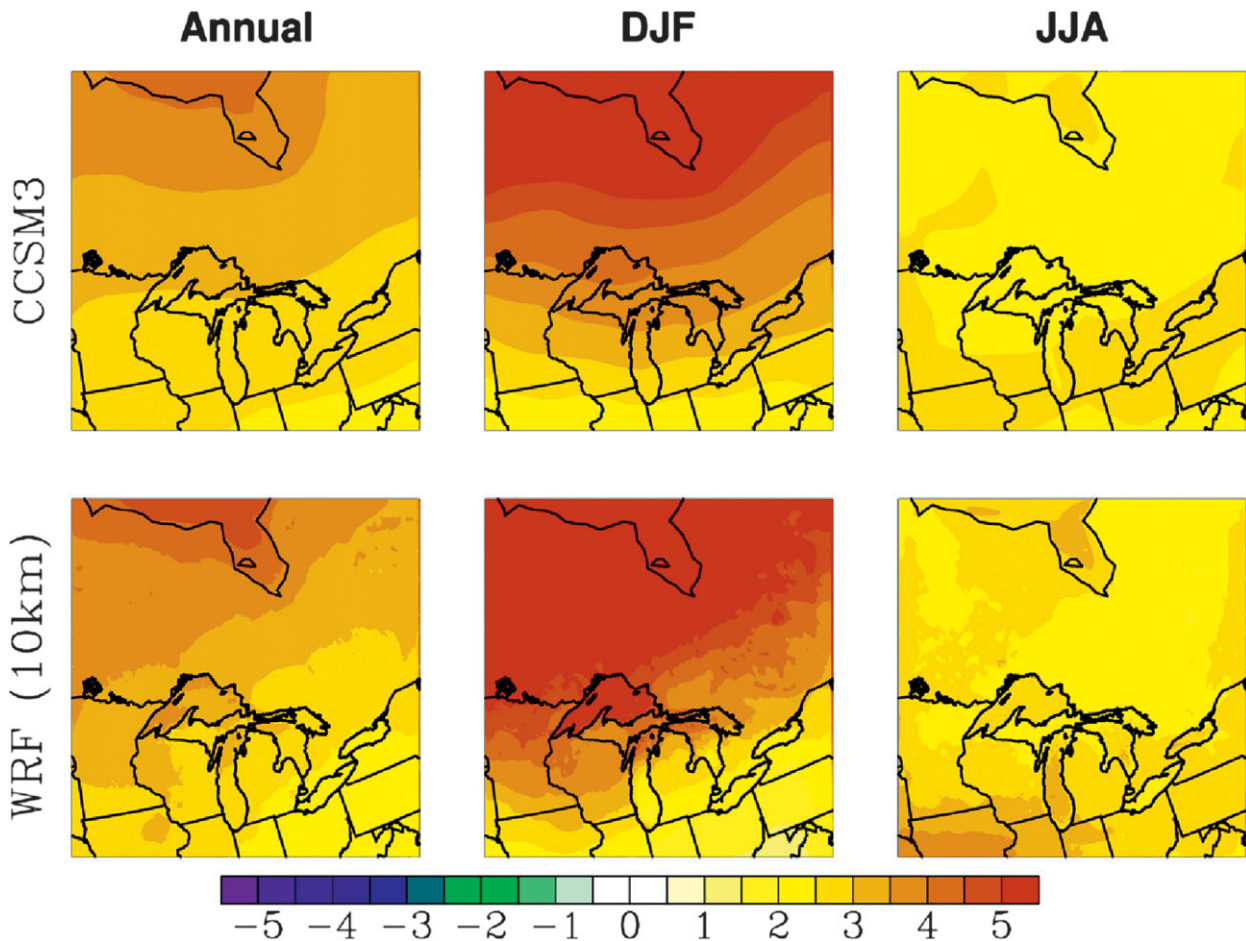


FIG. 10. Changes for the 2050–60 period relative to the historical period (1979–2001) over Ontario for (left) annual, (middle) winter, and (right) summer T_{mean} from the (top) CCSM and (bottom) WRF simulations.

shows a 15%–25% annual increase for most parts of the domain, changes are much more distinctive in the results of the WRF simulation. Mean annual precipitation shows less spatially coherent changes of smaller magnitude and of mixed sign. The response is especially different in the southeast portion of the domain where no change or a small decrease over Lakes Erie and Ontario and their surroundings is projected. The annual cycles of temperature, evaporation, precipitation, and snowfall as simulated by WRF over the Great Lakes Basin are shown in Fig. 12 for the 2050–60 and 1979–2001 periods. The increase in temperature translates into enhanced evaporation in late winter and spring, with subsequent increasing precipitation during the same period, while the late summer and fall are projected to experience a net drying. The projected changes in snowfall show a decrease at all times, as one would expect with increasing temperature and less frequent freezing days. These changes are stronger (up to a 20% decrease) during the first half of the cold season, from September

to January, while the second half, from late January to April, is characterized by a smaller decrease (around 10%).

Figure 13 shows a comparison of the annual change in snowfall for the CCSM and WRF simulations. A global decrease of snowfall by about 20%–30% is projected in the area for CCSM, which is consistent with the global warming trend over the region. However the changes in WRF are much more pronounced. The greatest differences are seen in the snowbelts, downwind of the Great Lakes, where in WRF the amount of snowfall is predicted to stay the same or at least undergo a smaller decrease.

Snowfall typically increases with decreasing temperature, and lake-effect snowfall also increases with decreasing temperature, but only until the lake becomes cold enough to freeze. At that point the ice shuts off evaporation, which prevents condensation and precipitation from occurring. In turn, lake-effect snow can increase with increasing temperature until it begins to fall when the temperature gradient becomes overly

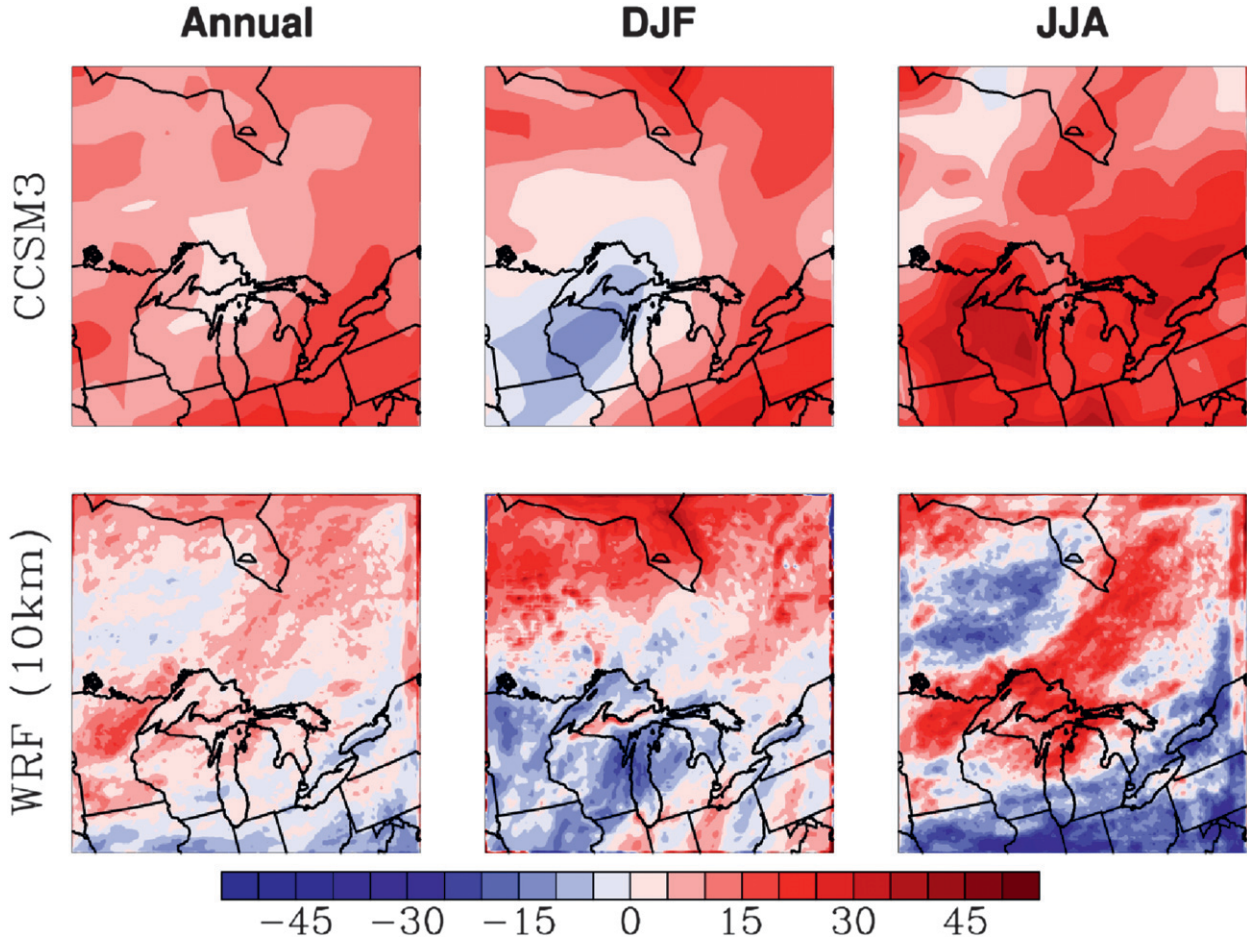


FIG. 11. Projected future changes of (left) annual, (middle) winter, and (right) summer mean precipitation (%) for the 2050–60 period relative to the historical period (1979–2001) over Ontario from (top) CCSM and (bottom) WRF.

strong. The decrease in snowfall due to the increasing temperature is then balanced in WRF by the diminution of ice cover and earlier warming of the lakes, which results in a longer period of unstable atmosphere and lake-effect precipitation. This is one of the most interesting results of the analyses we have performed.

Figure 14 shows the annual cycles of ice cover, temperature gradient, heat fluxes, and boundary layer height averaged over Lake Erie and Lake Superior. Annual cycles of precipitation and snowfall averaged over the corresponding snowbelts of these two lakes are also plotted in Fig. 14. For all lakes the diminution of ice cover results in an increase of the temperature gradient between the water temperature at the surface of the lakes and the atmosphere, the sensible and latent heat fluxes, and subsequently the height of the boundary layer above the lakes during winter, which are all favorable conditions for lake-effect snow. As can be seen in Fig. 14, these changes are more important for large

and deep lakes such as Lake Superior than for the shallow Lake Erie.

For the area as a whole, precipitation increases during spring and decreases during summer. One difference from the averaged domain precipitation is seen during late fall when the later freeze-up of the lakes extends the lake-effect rain period with local increase of rain precipitation in the snowbelt areas. The fall and early winter, from September to December, show an overall decrease in snowfall which is similar for all the snowbelt areas as well as for the whole Great Lakes Basin, directly related to the shift in temperature. But from mid-January to mid-March, a significant contrast appears between the snowbelts and the other parts of the domain. While most of the areas outside of the snowbelts continue to experience a drop in snowfall (Fig. 12), a different response is observed in the snowbelts themselves, from no change for the Lake Erie snowbelt to an increase for the Lake Superior snowbelt during this period.

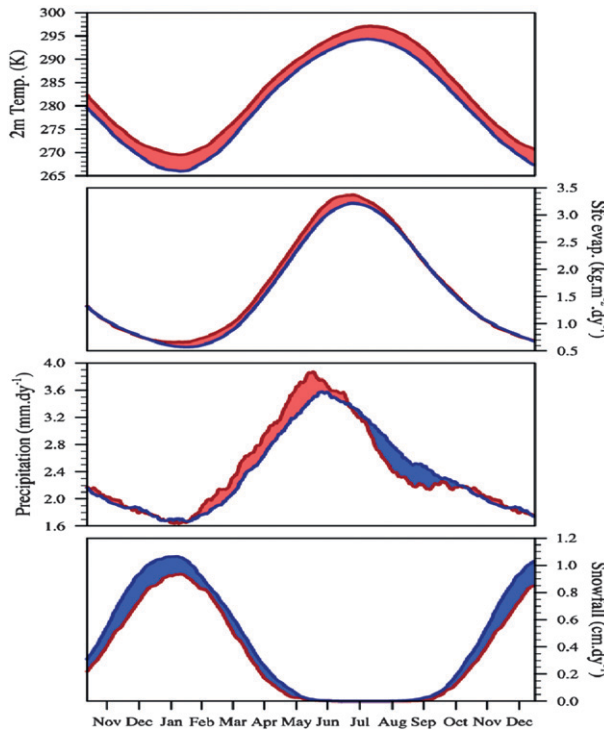


FIG. 12. Mean annual cycle for the 2050–60 period (red line) and the 1979–2001 period (blue line) averaged over the Great Lakes Basin for temperature at 2 m (K), surface evaporation (kg m^{-2}), total precipitation (mm day^{-1}), and snowfall (cm day^{-1}) from WRF. The area between the two lines is filled in red for positive differences (increase for the future period compared to the historical period) and in blue for negative differences.

Figure 15 shows changes in ice cover, temperature, heat fluxes, snowfall, and precipitation for the WRF simulation for January and February. A large increase is seen for the sensible and latent heat fluxes over the parts

of the lakes that used to be entirely covered by ice but remain more often ice free during the 2050–60 period. Changes are smaller for Lake Ontario and the deepest parts of Lakes Huron and Michigan, which were already seldom covered by ice during the historical period (see Fig. 3). These enhanced fluxes induce more precipitation and snowfall in the lee of the five Great Lakes during this period. These changes follow the trends observed in recent studies of snowfall records for the twentieth century (Burnett et al. 2003; Kunkel et al. 2009) and show that the increase in temperature is partially compensated by the reduced extent of ice cover, which enhances the lake effect. However, one can expect that as the temperature will further warm, the lake effect will still be enhanced but mostly in the form of rainfall as freezing conditions will not persist for a sufficient period of time.

5. Conclusions

The Weather Research and Forecasting model (WRF) has been employed to dynamically downscale global warming projections produced using the Community Climate System Model (CCSM) over the Great Lakes Basin at a spatial resolution of 10 km. Lake water temperature provided by the freshwater lake model “FLake” forced by atmospheric fields from the global simulations have been used in the WRF simulations to account for the influence of the Great Lakes.

Results for the present climate (1979–2001) have been compared to observations to evaluate the ability of the FLake model to provide accurate lake water temperature and ice cover and to analyze the skill of the WRF regional climate model. The FLake model, despite its relative simplicity and unavoidable biases derived from

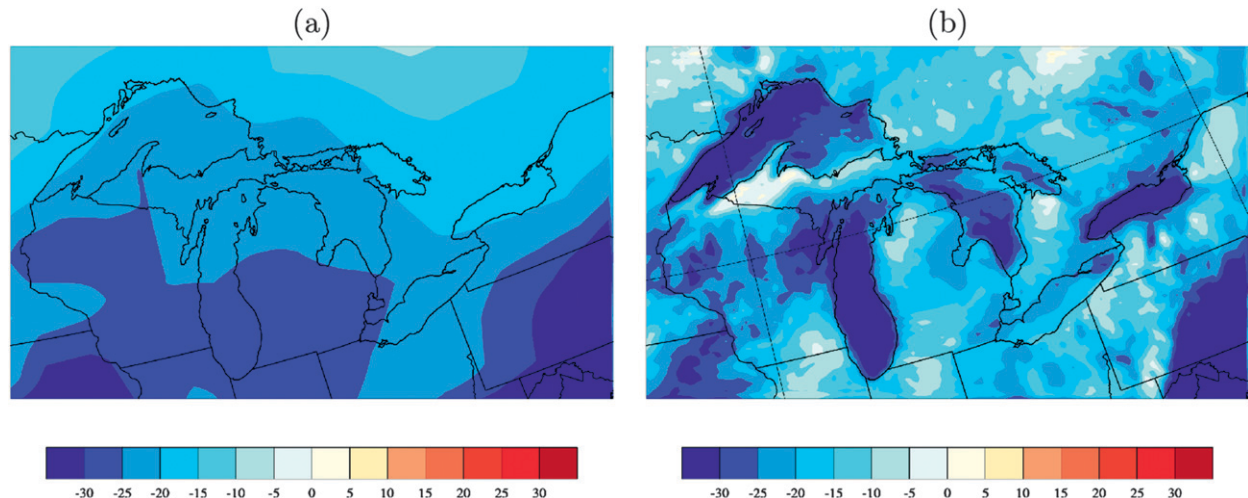


FIG. 13. Changes for the 2050–60 period relative to the historical period (1979–2001) over the Great Lakes Basin for snow precipitation (%) from (a) CCSM and (b) WRF.

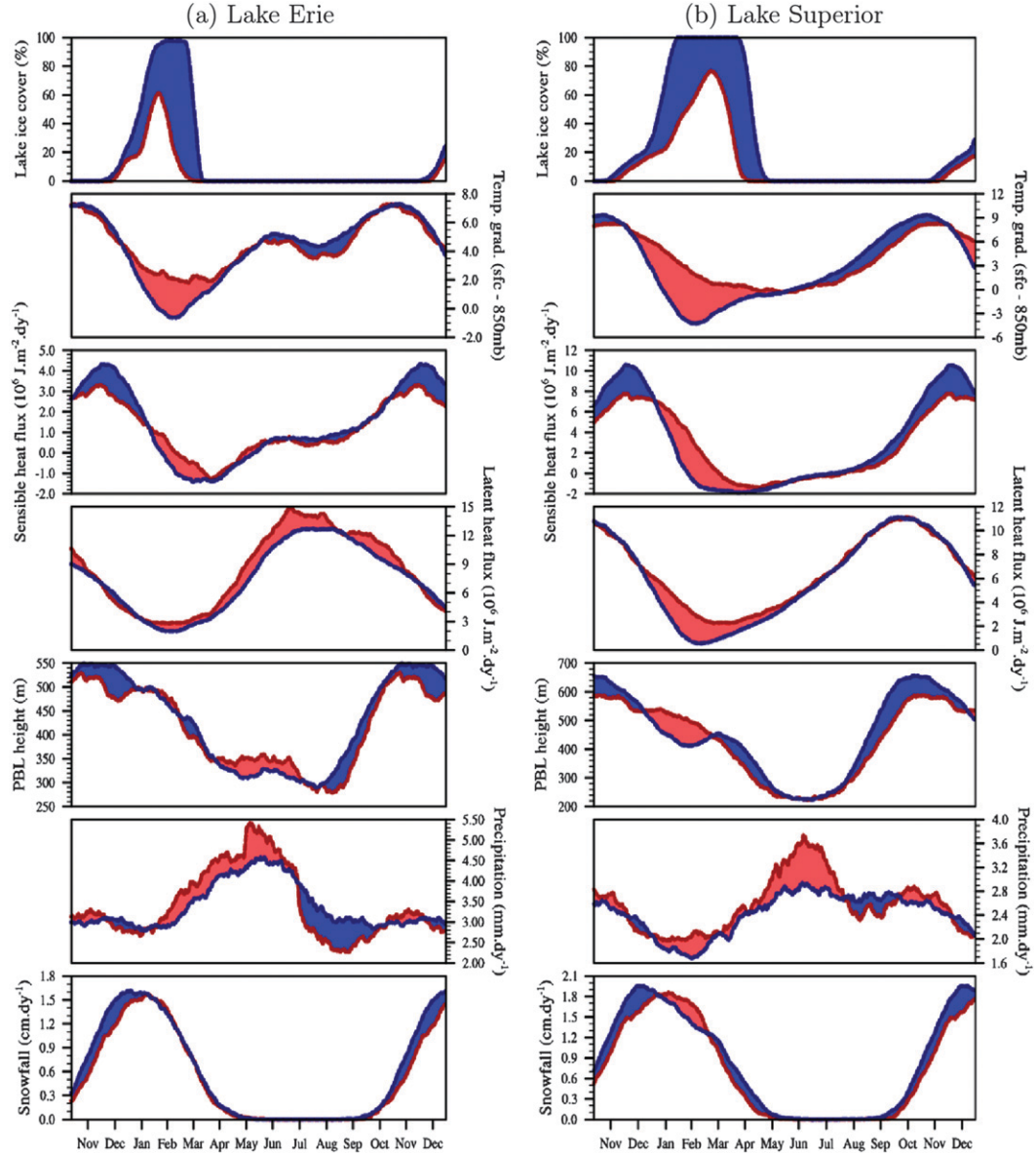


FIG. 14. Mean annual cycle from WRF for the 2050–60 period (red dashed line) and the 1979–2001 period (blue dashed line) for the lake ice cover (in percent of the lake surface), temperature difference between surface and 850-mb isobar, sensible heat flux, and latent heat flux averaged over the lake surface for (a) Lake Erie and (b) Lake Superior; and for the rain and snowfall averaged over the corresponding snowbelt areas (see Fig. 7).

our use of the forcing CCSM atmospheric fields, is able to reproduce reasonably most features of the temporal evolution and the spatial patterns of lake water temperature and ice cover over the Great Lakes. The main discrepancies are observed in the deepest part of Lake Superior where the 1D formulation of the model is not able to fully account for the more complex dynamics of the lake and its influence on the evolution of lake temperature.

The methodology has proven able to much more accurately reproduce known features of the regional climate

over the historical period. The WRF downscaled results show improved skill in simulating surface air temperature. The main difference is seen in the vicinity of the Great Lakes, where the regional thermal moderation provided by the Great Lakes system is considerably improved when compared to the large-scale CCSM results. The ability of the model to reduce biases and increase correlation is more striking for precipitation and snowfall, especially in the lee of the lakes where lake-enhanced precipitation is simulated more realistically.

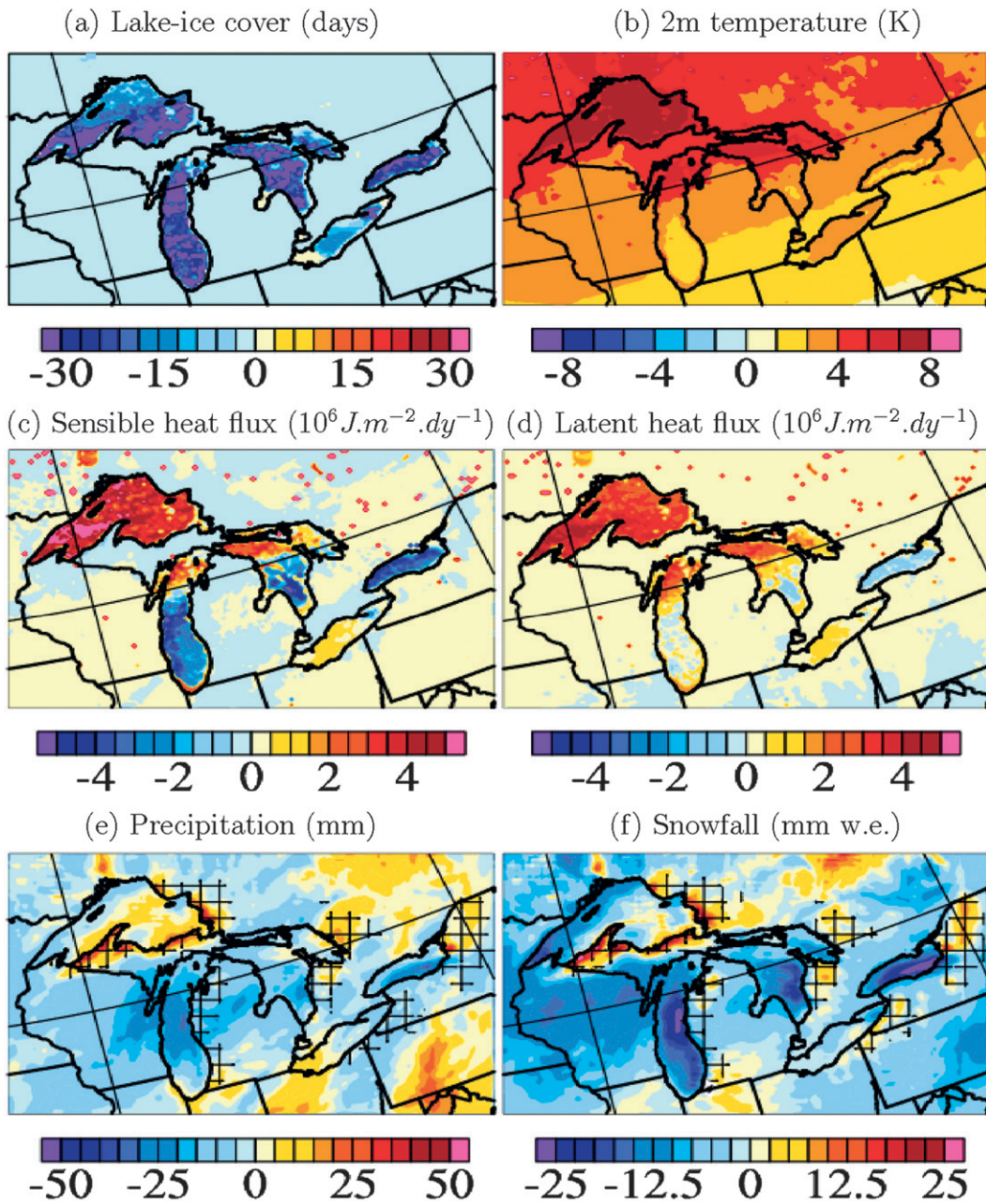


FIG. 15. Mean changes for January and February from WRF for the 2050–60 period compared to the 1979–2001 period for (a) lake ice cover, (b) temperature at 2 m, (c) sensible heat flux, (d) latent heat flux, (e) total precipitation, and (f) snowfall. The filled areas correspond to the snowbelt location computed from historical snowfall (see Fig. 7).

A midcentury (2050–60) projection has been analyzed in detail to determine the impact of downscaling on regional climate changes. Changes in lake water temperatures and ice cover have been shown to exert a highly significant impact on the spatial and seasonal variations of precipitation, especially in the lee of the lakes where local changes are strongly influenced by lake–atmosphere interactions. It has been found that future changes in lake

surface temperature and ice cover under warmer conditions may locally increase snowfall as a result of increased evaporation and the enhanced lake effect.

These results provide substantial evidence that mesoscale processes play an important role in the local response to climate change in the region of the Great Lakes. Further advanced regional climate modeling studies for the region will be critical to understanding

the regional impacts of global climate change. While results shown in this study are limited to a single scenario from a single global model, these fundamental results depend on physical mechanisms that appear to be robust. Simulations using the WRF model with alternative microphysics, cumulus parameterizations, and surface and planetary boundary layer schemes, as well as different nudging parameters, which are not shown in this study, have been performed following the same methodology. Summer precipitation amplitude and patterns have been found to be extremely sensitive to the various parameterizations but no significant differences were found for processes related to the winter precipitation and snowfall in the lee of the lakes.

Further work is needed to improve the model so as to more accurately account for the influence of the Great Lakes. In particular the methodology presented here does not account for atmosphere–lake feedbacks, which would likely further increase the impact of the lakes on the regional climate. Preliminary results have been obtained using a further improved version of the methodology in which FLake is fully coupled to WRF. Modifications to the projections described in this paper appear to be modest and do not undercut the primary conclusions presented herein, but must be further analyzed to better understand the impact of the Great Lakes on regional greenhouse warming.

Acknowledgments. The work described in this paper was partially funded by the Ontario Ministry of the Environment and by NSERC Discovery Grant A9627 to WRP. The computations upon which the paper is based were performed on the University of Toronto SciNet facility for High Performance Computation, which is a component of the Compute Canada HPC platform.

REFERENCES

- Assel, R., 1986: Fall and winter thermal structure of Lake Superior. *J. Great Lakes Res.*, **12**, 251–262.
- , 2003: Great Lakes ice cover, first ice, last ice, and ice duration: Winters 1973–2002. NOAA Tech. Memo. GLERL-125, 49 pp. [Available online at http://www.glerl.noaa.gov/ftp/publications/tech_reports/glerl-125/tm-125.pdf.]
- Austin, J., and S. Colman, 2007: Lake Superior summer water temperatures are increasing more rapidly than regional air temperatures: A positive ice-albedo feedback. *Geophys. Res. Lett.*, **34**, L06604, doi:10.1029/2006GL029021.
- Beletsky, D., and D. Schwab, 2001: Modeling circulation and thermal structure in Lake Michigan: Annual cycle and interannual variability. *J. Geophys. Res.*, **106** (C7), 19 745–19 771.
- Boyce, F., M. Donelan, P. Hamblin, C. R. Murthy, and T. Simons, 1989: Thermal structure and circulation in the Great Lakes. *Atmos.–Ocean*, **27**, 607–642.
- Brown, L., and C. Duguay, 2010: The response and role of ice cover in lake–climate interactions. *Prog. Phys. Geogr.*, **34**, 671–704.
- Bukovsky, M., and D. Karoly, 2008: An evaluation of climate model precipitation over the United States. *Preprints, 20th Conf. on Climate Variability and Change*, New Orleans, LA, Amer. Meteor. Soc., P3.8. [Available online at <https://ams.confex.com/ams/88Annual/webprogram/Paper134940.html>.]
- Burnett, A., M. Kirby, H. Mullins, and W. Patterson, 2003: Increasing Great Lake effect snowfall during the twentieth century: A regional response to global warming? *J. Climate*, **16**, 3535–3542.
- Chen, F., and J. Dudhia, 2001: Coupling an advanced land surface–hydrology model with the Penn State–NCAR MM5 modeling system. Part I: Model implementation and sensitivity. *Mon. Wea. Rev.*, **129**, 569–585.
- Davies, H., and R. E. Turner, 1977: Updating prediction models by dynamical relaxation: An examination of the technique. *Quart. J. Roy. Meteor. Soc.*, **103**, 225–245.
- Devine, K., and E. Mekis, 2008: Field accuracy of Canadian rain measurements. *Atmos.–Ocean*, **46**, 213–227.
- Fita, L., J. Fernández, and M. García-Díez, cited 2009: CLWRF: WRF modifications for regional climate simulation under future scenarios. *Proc. 11th WRF Users' Workshop*, Boulder, CO, NCAR. [Available online at http://www.meteo.unican.es/files/pdfs/WRFusers_elwrf.pdf.]
- Fowler, H., S. Blenkinsop, and C. Tebaldi, 2007: Linking climate change modelling to impacts studies: Recent advances in downscaling techniques for hydrological modelling. *Int. J. Climatol.*, **27**, 1547–1578.
- Giorgi, F., 2006: Regional climate modeling: Status and perspectives. *J. Phys. IV*, **139**, 101–118.
- Held, I., and B. Soden, 2006: Robust responses of the hydrological cycle to global warming. *J. Climate*, **19**, 5686–5699.
- Hong, S.-Y., J. Dudhia, and S.-H. Chen, 2004: A revised approach to ice microphysical processes for the bulk parameterization of clouds and precipitation. *Mon. Wea. Rev.*, **132**, 103–120.
- Hostetler, S., G. Bates, and F. Giorgi, 1993: Interactive coupling of a lake thermal model with a regional climate model. *J. Geophys. Res.*, **98** (D3), 5045–5057.
- , F. Giorgi, G. Bates, and P. Bartlein, 1994: Lake–atmosphere feedbacks associated with paleolakes Bonneville and Lahontan. *Science*, **263**, 665–668.
- Kitaigorodskii, S., and Y. Miropolsky, 1970: On the theory of the open ocean active layer. *Izv. Atmos. Ocean. Phys.*, **6**, 178–188.
- Kourzeneva, E., 2009: Global dataset for the parameterization of lakes in numerical weather prediction and climate modeling. *ALADIN Newsletter*, No. 37, ALADIN, Toulouse, France, 46–53.
- Kunkel, K., L. Ensor, M. Palecki, D. Easterling, D. Robinson, K. Hubbard, and K. Redmond, 2009: A new look at lake-effect snowfall trends in the Laurentian Great Lakes using a temporally homogeneous data set. *J. Great Lakes Res.*, **35**, 23–29.
- Leung, L., Y. Qian, and X. Bian, 2003: Hydroclimate of the western United States based on observations and regional climate simulations of 1981–2000. Part I: Seasonal statistics. *J. Climate*, **16**, 1892–1911.
- Liang, X.-Z., J. Pan, J. Zhu, K. Kunkel, J. Wang, and A. Dai, 2006: Regional climate model downscaling of the U.S. summer climate and future change. *J. Geophys. Res.*, **111**, D10108, doi:10.1029/2005JD006685.
- , K. E. Kunkel, G. Meehl, R. Jones, and J. Wang, 2008: Regional climate models downscaling analysis of general circulation models present climate biases propagation into future change projections. *Geophys. Res. Lett.*, **35**, L08709, doi:10.1029/2007GL032849.
- Lo, J.-F., Z.-L. Yang, and R. A. Pielke Sr., 2008: Assessment of three dynamical climate downscaling methods using the Weather

- Research and Forecasting (WRF) model. *J. Geophys. Res.*, **113**, D09112, doi:10.1029/2007JD009216.
- Martynov, A., L. Sushama, and R. Laprise, 2010: Simulation of temperate freezing lakes by one-dimensional lake models: Performance assessment for interactive coupling with regional climate models. *Boreal Environ. Res.*, **15**, 143–164.
- Mekis, E., and W. Hogg, 1999: Rehabilitation and analysis of Canadian daily precipitation time series. *Atmos.–Ocean*, **37**, 53–85.
- Mesinger, F., 2006: North American Regional Reanalysis. *Bull. Amer. Meteor. Soc.*, **87**, 343–360.
- Miguez-Macho, G., G. L. Stenchikov, and A. Robock, 2004: Spectral nudging to eliminate the effects of domain position and geometry in regional climate model simulations. *J. Geophys. Res.*, **109**, D13104, doi:10.1029/2003JD004495.
- Mironov, D., 2008: Parameterization of lakes in numerical weather prediction: Description of a lake model. COSMO Tech. Rep. 11, 41 pp.
- , E. Heise, E. Kourzeneva, B. Ritter, N. Schneider, and A. Terzhevik, 2010: Implementation of the lake parameterisation scheme FLake into the numerical weather prediction model COSMO. *Boreal Env. Res.*, **15**, 218–230.
- Mishra, V., K. Cherkauer, L. Bowling, and M. Huber, 2011: Lake ice phenology of small lakes: Impacts of climate variability in the Great Lakes region. *Global Planet. Change*, **76**, 166–185.
- Mitchell, T., and P. Jones, 2005: An improved method of constructing a database of monthly climate observations and associated high-resolution grids. *Int. J. Climatol.*, **25**, 693–712.
- Nakicenovic, N., and R. Swart, 2000: *Emissions Scenarios*. Cambridge University Press, 599 pp.
- New, M., D. Lister, M. Hulme, and I. Makin, 2002: A high-resolution data set of surface climate over global land areas. *Climate Res.*, **21**, 1–25.
- Noh, Y., W. G. Cheon, S.-Y. Hong, and S. Raasch, 2003: Improvement of the K-profile model for the planetary boundary layer based on large eddy simulation data. *Bound.-Layer Meteor.*, **107**, 401–427.
- Reynolds, R., T. Smith, C. Liu, D. Chelton, K. Casey, and M. Schlax, 2007: Daily high-resolution blended analyses for sea surface temperature. *J. Climate*, **20**, 5473–5496.
- Rudolf, B., C. Beck, J. Grieser, and U. Schneider, cited 2005: Global precipitation analysis products. Global Precipitation Climatology Centre (GPCC). [Available online at <http://gpcc.dwd.de/>.]
- Scott, R., and F. Huff, 1996: Impacts of the Great Lakes on regional climate conditions. *J. Great Lakes Res.*, **22**, 845–863.
- Skamarock, W., J. Klemp, J. Dudhia, D. Gill, D. Barker, W. Wang, and J. G. Powers, 2007: A description of the Advanced Research WRF version 2. NCAR Tech. Note NCAR/TN-468+STR, 88 pp.
- Solomon, S., D. Qin, M. Manning, Z. Chen, M. Marquis, K. Averyt, M. Tignor, and H. Miller, Eds., 2007: *Climate Change 2007: The Physical Science Basis*. Cambridge University Press, 996 pp.
- Trenberth, K., A. Dai, R. Rasmusson, and D. Parsons, 2003: The changing character of precipitation. *Bull. Amer. Meteor. Soc.*, **84**, 1205–1217.
- Vincent, L., and E. Mekis, 2006: Changes in daily and extreme temperature and precipitation indices for Canada over the twentieth century. *Atmos.–Ocean*, **44**, 177–193.
- , and —, 2009: Discontinuities due to joining precipitation station observations in Canada. *J. Appl. Meteor. Climatol.*, **48**, 156–166.
- Wang, Y., L. Leung, J. McGregor, D. Lee, W. Wang, Y. Ding, and F. Kimura, 2004: Regional climate modeling: Progress, challenges, and prospects. *J. Meteor. Soc. Japan*, **82**, 1599–1628.
- Zheng, X., M. Shaikh, Y. Dai, R. Dickinson, and R. Myneni, 2002: Coupling of the Common Land Model to the NCAR Community Climate Model. *J. Climate*, **15**, 1832–1854.